doi:10.3788/gzxb20164508.0826001

棱镜波导结构的古斯-汉欣位移模拟

张文静,张志伟,杨鹏,朱祥,戴一帆,魏玉芸
(中北大学 信息与通信工程学院,太原 030051)

摘 要:模拟并分析了波长为 633 nm 的偏振光通过 Kretschmann-Raether 微米级棱镜波导结构时的古斯-汉欣位移.在金膜厚度为 45 nm 的条件下,当入射角为 44.1°时,利用稳态相位理论,得到的最大束位移为+120 μm;当入射角为 44.1°时,利用 COMSOL Multiphysics5.1 软件中的波动光学模块,得到的最大束位移为+3.37 μm.在共振角附近,COMSOL Multiphysics5.1 模拟软件与稳态相位理论均得到正的古斯-汉欣位移,但是 COMSOL Multiphysics5.1 软件模拟的结果远小于稳态相位理论仿真的结果.该研究对设计基于古斯-汉欣位移测量的高灵敏度传感器具有指导意义.

关键词:集成光学;表面等离子体共振;古斯-汉欣位移;非线性光学
中图分类号:O436 **文献标识码**:A **文章编号**:1004-4213(2016)08-0826001-6

Goos-Hänchen Shifts Around the Resonance Angle of a Prism Waveguide Structure

ZHANG Wen-jing, ZHANG Zhi-wei, YANG Peng, ZHU Xiang, DAI Yi-fan, WEI Yu-yun
(*School of Information and Communication Engineering, North University of China, Taiyuan*, 030051, *China*)

Abstract: Goos-Hänchen (GH) shifts of 633 nm polarized light through a μm-order isosceles triangle prism waveguide structure with Kretschmann-Raether configuration were simulated and analyzed. When the thickness of gold film is 45 nm, the maximum positive beam displacement, obtained using a Stationary-Phase Analysis (SPA), is about +120 μm at the incident angle of 44.1°; and it is +3.37 μm using COMSOL Multiphysics5.1 (CM) at the incident angle of 44.1°. The beam displacements, obtained using CM and SPA around the resonance angle, are all positive, although the enhancement effect from CM is much less than that of SPA. These results are useful for designing high sensitivity sensors based on GH shift measurement.

Key words: Integrated optics devices; Surface plasmons resonance; Goos-Hänchen shifts; Nonlinear optics at surfaces
OCIS Codes: 260.1960; 260.2065; 260.6970; 130.3120; 240.6680; 240.4350

0 Introduction

When a light beam undergoes the Total Internal Reflection (TIR) from a dielectric interface, between an optically dense medium and an optically thin medium, the reflected light beam is laterally shifted away from the incident beam by a very small amount. This phenomenon, known as the Goos-Hänchen (GH) shift, was experimentally demonstrated by Goos and Hänchen in 1947[1]. The GH shift depends on the polarization state of the incident beam, i.e., GH shift in the plane of incidence is different depending on whether light is TM-polarized or TE-polarized. The Fresnel formulae have been used to derive theoretical methods, including energy conservation models[2] and stationary phase models[3], and to calculate the optical

Foundation item: The National Natural Science Foundation (Youth) of China (No. 11304289)
First author: ZHANG Wen-jing (1989—), female, Ph.D. degree candidate, mainly focuses on the optical heterodyne communication and application. Email:736272126@qq.com
Supervisor(Corresponding author): ZHANG Zhi-wei (1964—), male, professor, Ph.D. degree, mainly focuses on plasmonics and optical sensor technology. Email:zhangzwei@nuc.edu.cn
Received: Mar. 14, 2016; **Accepted**: Jun. 3, 2016

beam displacement in the incident plane for TM and TE polarization states. However, the magnitude of GH shift for TIR is about the order of the optical wavelength, the smallness of which can impede its direct measurement and application[4]. To enhance GH shift and make measurement easier, the beam was reflected multiple times, but this method is not convenient for the application of GH shift. In addition, the GH shift can be enhanced for TIR by a single thin-film for TM and TE polarized lights[5] or for TM polarized light at the metal surface due to the Surface Plasmon Resonance (SPR)[6-7]. SPR is a charge-density oscillation that may occur between two media with dielectric constants of opposite signs, such as a metal and a dielectric[8]. SPR can be generated when TM polarized light is launched into a prism coated with a thin-film metal, and the reflected light has a GH shift along the metal interface. The GH shift on the SPR is attributed to the phase changes of the reflected light[9]. Ref. [9] has explicated GH shift of a μm-order Kretschmann-Raether configuration embedded in an optical waveguide structure by using the finite-difference time-domain method. For example, when the thickness of the gold film is 50 nm, the accurate positive and negative GH shifts of +1.0 and −0.75 μm are respectively obtained on the SPR with the incident angles of 47.5° and 44.4° at a wavelength of 632.8 nm.

In this paper, for a μm-order prism waveguide structure with Kretschmann-Raether configuration, the critical thickness of 45.8 nm is found for gold film. When the thickness of the gold film is 45 nm, the maximum positive beam displacements of about +120 μm is obtained around the resonance angle of 44.1° by using a Stationary-Phase Analysis (SPA), at a wavelength of 633 nm. We use the COMSOL Multiphysics5.1 (CM) for simulating and analyzing GH shift around the resonance angle in more detail. The maximum positive beam displacements of +3.37 μm is found at an incident angle of 44.1°. The beam displacements are positive around the resonance angle, these results are in good agreement with that of Ref. [6].

1 Goos-Hänchen shift

The fundamental principle geometry of a prism enhanced GH shift at SPR is shown in Fig. 1[10-11], where P is the isosceles prism with gold film deposited on its bottom; the dash line is the geometrical reflection ray for a prism without a gold film at the bottom, the solid lines with arrows represent the light paths; the gold thin film (with complex permittivity $\varepsilon_2=\varepsilon_{2r}+i\varepsilon_{2i}$) with thickness d is the interface between prism P (permittivity ε_1) and the sample (dielectric medium with permittivity ε_3, where $\varepsilon_3<\varepsilon_1$); the s is the enhanced beam displacement and Δ is GH shift. Prism P, the gold film, and the dielectric medium are assumed to be nonmagnetic ($\mu_r=1$). In general, the GH shift occurs in the positive lateral direction along the interface in the incident plane.

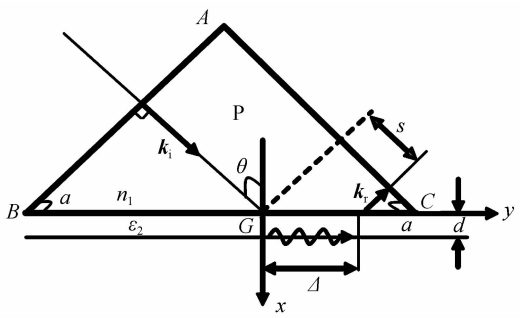

Fig. 1 Schematic diagram of the three-layer system

We assume that TM-polarized light is normal to surface AB of the isosceles prism P onto its bottom at the incident angle, $\theta>\arcsin(n_s/n_1)$, where θ is equal to base angle α of prism. The vector $\boldsymbol{k}_i$, which denotes the propagation of TM-polarized light, is in the plane of the diagram shown in Fig. 1. Let $\boldsymbol{E}_{ip}$ be the electric vector of the incident TM-polarized light. $\boldsymbol{E}_{ip}$ is totally reflected at the P-gold interface, evanescently penetrates through the gold film and excites Surface Plasmon Waves (SPWs) at the outer boundary of the gold film[12]. The optical excitation of a SPW results in the SPR, while GH shift (Δ) is greatly enhanced. The GH shift can be detected by changes in the reflect electric field (E-field) $\boldsymbol{E}_{rp}$. As shown in Eq. (1), the vector $\boldsymbol{E}_{rp}$ propagating in the direction of vector $\boldsymbol{k}_r$ are all E-fields in the reflected wave at the interfaces of P-gold and gold-sample, and it is the product of the complex reflection coefficient (r_1) and the incident E-field $\boldsymbol{E}_{ip}$[13].

$$\boldsymbol{E}_{rp}=r_1\boldsymbol{E}_{ip}=\rho_1 e^{-i\delta_{1r}}\boldsymbol{E}_{ip} \tag{1}$$

where $\delta_{1r}=\delta_{1r}(\lambda,\theta,n_s,d)$ denotes the phase term, λ is the optical wavelength, n_s is the refractive index of the sample (where $n_s=\varepsilon_s^{1/2}$), d is the gold film thickness and $\rho_1=\rho_1(\lambda,\theta,n_s,d)$ is the amplitude. The complex reflection coefficient is comprised of both ρ_1 and δ_{1r}.

For the three-layer configuration shown in Fig. 1, the complex reflection coefficient r_1 at point G, on the basis of multilayer electro-magnetic theory[14-16], can be expressed as

$$r_1=\frac{r_{12}+r_{23}\exp(i2k_{2x}d)}{1+r_{12}\cdot r_{23}\exp(i2k_{2x}d)}=\rho_1 e^{i\delta_{1r}} \tag{2}$$

where r_{12} and r_{23} are the reflection coefficients at the P-gold and gold-sample interfaces, respectively. δ_{1r} is the reflection phase change at point G. For TM-polarized

light

$$r_{ij}=\frac{(k_{ix}/\varepsilon_i)-(k_{jx}/\varepsilon_j)}{(k_{ix}/\varepsilon_i)+(k_{jx}/\varepsilon_j)},i=1,2 \text{ and } j=2,3 \quad (3)$$

where $k_{ix}=\sqrt{k_i^2-k_y^2}$, $k_i=k\sqrt{\varepsilon_i}$ $(i=1,2,3)$, $k_y=k\sqrt{\varepsilon_1}\sin\theta$, $k_{2x}=u_2+\mathrm{i}v_2$, $r_{12}=\rho_{12}\exp(\mathrm{i}\varphi_1)$, $r_{23}=\rho_{23}\exp(\mathrm{i}\varphi_2)$, $k=2\pi/\lambda$ is the wave number in the vacuum. From Eqs. (2) and (3), we can obtain the reflectance R and the phase change δ_{1r} from the following expressions[14]

$$R=|r_1|^2=[\rho_{12}^2\mathrm{e}^{2v_2d}+\rho_{23}^2\mathrm{e}^{-2v_2d}+2\rho_{12}\rho_{23}\cos(\varphi_2-\varphi_1+2u_2d)]/[\mathrm{e}^{2v_2d}+\rho_{12}^2\rho_{23}^2\mathrm{e}^{-2v_2d}+2\rho_{12}\rho_{23}\cdot\cos(\varphi_1+\varphi_2+2u_2d)] \quad (4)$$

$$\tan\delta_{1r}=[\rho_{23}(1-\rho_{12}^2)\sin(2du_2+\varphi_2)+\rho_{12}(\mathrm{e}^{2v_2d}-\rho_{23}^2\mathrm{e}^{-2v_2d})\sin\varphi_1]/[\rho_{23}(1+\rho_{12}^2)\cos(2du_2+\varphi_2)+\rho_{12}(\mathrm{e}^{2v_2d}+\rho_{23}^2\mathrm{e}^{-2v_2d})\cos\varphi_1] \quad (5)$$

We note that the total reflection of the incident beam into prism P is not only due to the gold-sample interface, since the P-gold interface also affects the reflection. Thus, the GH shift of the totally reflected beam is defined as a lateral displacement of the beam, relative to the position predicted by geometrical reflection along the first interface, as is depicted in Fig. 1[4,7]. As shown in Fig. 1, the beam displacement (s) at SPR is given by[3]

$$s=\Delta\cos\theta=-\frac{1}{k_1}\frac{\mathrm{d}\delta_{1r}}{\mathrm{d}\theta}\Big|_{\theta=\theta_{SPR}} \quad (6)$$

where k_1 is the wave number in prism P, θ is the incident angle at points G, θ_{SPR} is the resonance angle at points G, and δ_{1r} is the phase difference between the reflected and incident light at point G.

2 Simulation results and discussion

Simulations are performed using the Kretschmann-Raether configuration and Eqs. (4), (5), and (6). Fig. 2 shows the dependence, on the incident angle, of the reflectivity and phase shift of TM-polarized components of reflected light, where $\varepsilon_1=2.2944$ (K9 glass), $\varepsilon_2=-10.92+\mathrm{i}1.49$ (gold), $\varepsilon_s=1.00025$ (air). The thickness of the gold film is 45 nm and the optical wavelength is 633 nm.

We notice in Fig. 2 that the reflectivity and phase shift for TM-polarized light excitation have an abrupt change around the resonance angle. The resonance angle for minimum reflectivity is 44.1°. The absorption curves of the reflectance and phase changes depend on the thickness of the gold film. Correspondingly, for TM-polarized light excitation, the enhanced beam displacement at the resonance angle, at different thicknesses of gold film, are shown in Fig. 3, the other parameters are the same as that used in Fig. 2. We notice that the beam displacement at resonance angle are positive at thicknesses of gold film of 43 nm, 44 nm, and 45 nm. While the thicknesses of gold film are 47 nm and 48 nm, the beam displacement become negative.

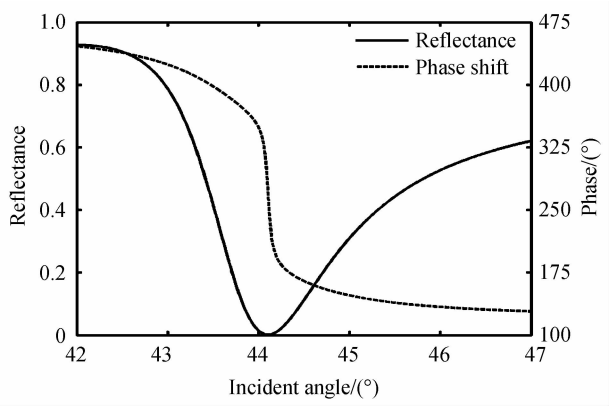

Fig. 2 Reflectivity and phase shift of TM-polarized light vs. the incident angle

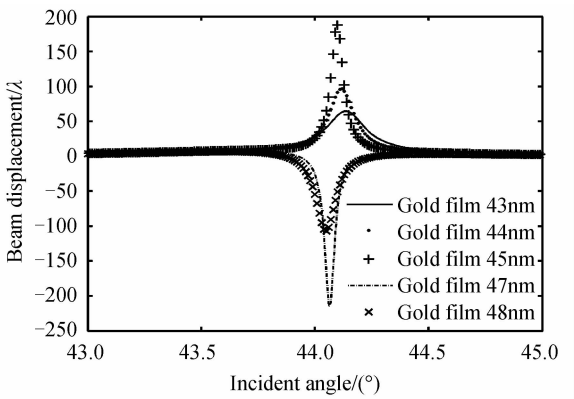

Fig. 3 Dependence of the beam displacement of TM-polarized light on the incident angle

Fig. 4 shows the dependence of the reflectivity on the thicknesses of gold film at the wavelength of 633 nm, the other parameters are the same as that used in Fig. 2. As shown in the figure, the thickness for a reflectivity minimum indicates the critical condition at which the negative direction beam displacement appears[6]. This thickness is also well known as optimal thickness for excitation of the surface plasmon[6], where the resonance absorption is just

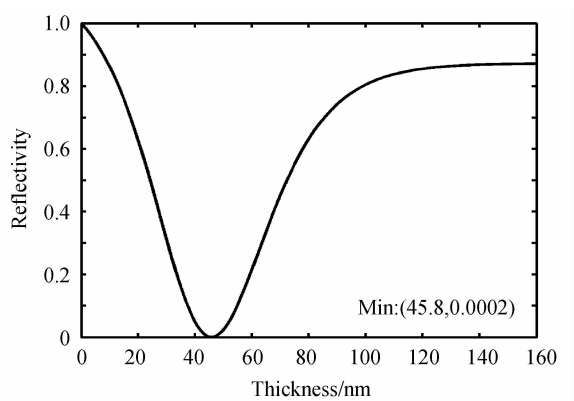

Fig. 4 Dependence of the reflectivity of TM-polarized light on the thicknesses of gold film

balanced by radiation damping and internal damping. We notice in Fig. 4 that the critical thickness is approximately 45.8 nm at the resonance angle of 44.1°. Furthermore, by comparing Figs. 3 and 4, we notice that the much larger beam displacement can be expected when the thickness is close to the critical thickness. In this study, we consider the resonance characteristic of the gold film of thickness 45 nm for TM-polarized light.

According to the configuration shown in Fig. 1, we obtain, from Eq. (5), the dependence of the phase shift of TM-polarized light on the incident angle in Fig. 2, where the thickness of gold film is 45 nm. We observe that the phase shift abruptly changes from 400° to 175° at the resonance angle. The result illustrates that the positive beam displacement increase at point G for incident TM-polarized light.

The phase shift diagram in Fig. 2 illustrates the curve of the beam displacement over the incident angle from Eq. (6). For example, for TM-polarized light, the beam displacement at point G in Fig. 1 as a function of the incident angle are shown in Fig. 5, where the wavelength is 633 nm and the gold film thickness is 45 nm, the other parameters are the same as that used in Fig. 2. In Fig. 5, we observe that the beam displacement sharply increases after a SPR excitation at the incident angle of 44.1°. The beam displacement can reach to an easily measurable quantity of about +120 μm.

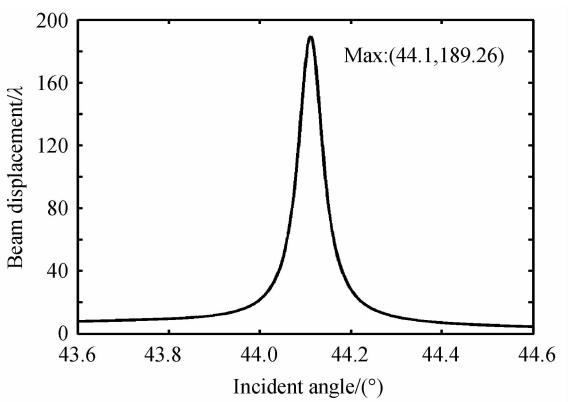

Fig. 5 Dependence of the beam displacement on the incident angle

As shown in Fig. 5, the beam displacement increases about +120 μm at the incident angle of 44.1°. This is because the effect of SPA is the differentiation of the phase shift with respect to the incident angle[9,17]. The CM software provides finite element analysis, a solver, and relevant simulation tools. Therefore, we can measure GH shifts in prism waveguide SPR sensor devices using wave optics model of CM. For example, for the isosceles triangle prism, at an incident angle of 44.1°, the optical-mode propagations analyzed by CM are shown in Fig. 6, the other parameters are the same as that used in Fig. 2.

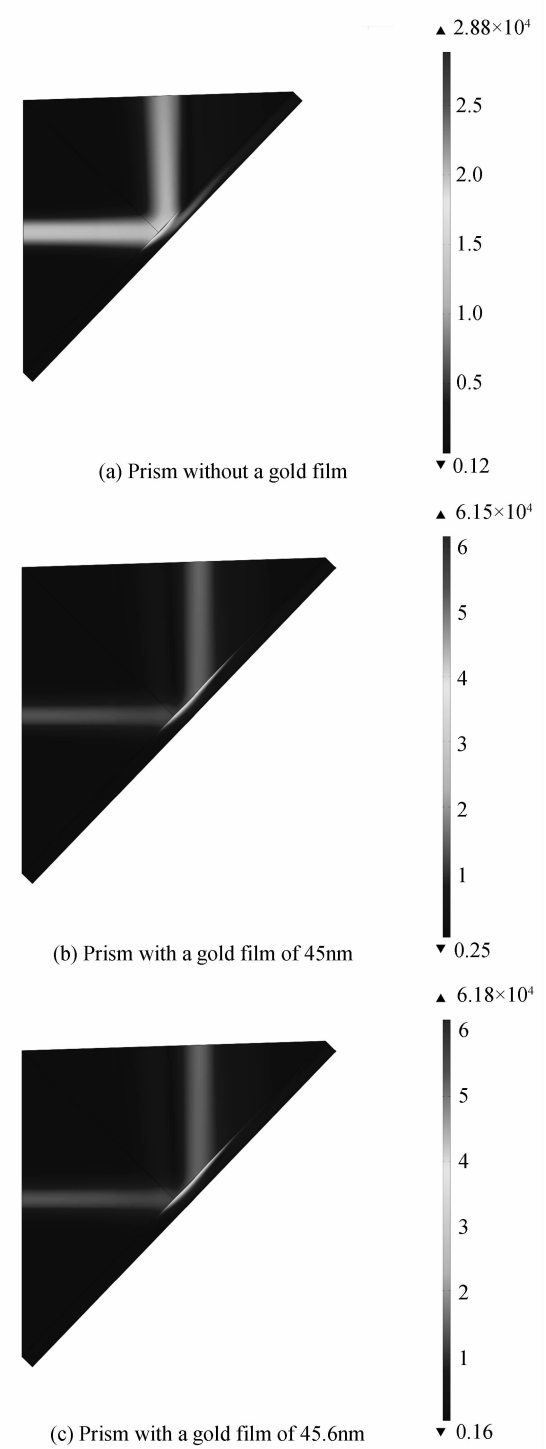

Fig. 6 Optical-mode propagations using CM

The E-field intensity distributions of optical-mode propagations for reflected light in Fig. 6 are shown in Fig. 7.

From Fig. 7, by comparing the position appeared the maximum E-field intensity at prism coated with a gold film with that of the prism without gold film, we can obtain the beam displacements are +3.37 μm and +3.67 μm, at the thicknesses of gold film of 45 nm

and 45.6 nm, respectively. When the thickness is close to 45.8 nm, the beam displacement is on the increase, but there is a great difference by comparison with effect from the SPA.

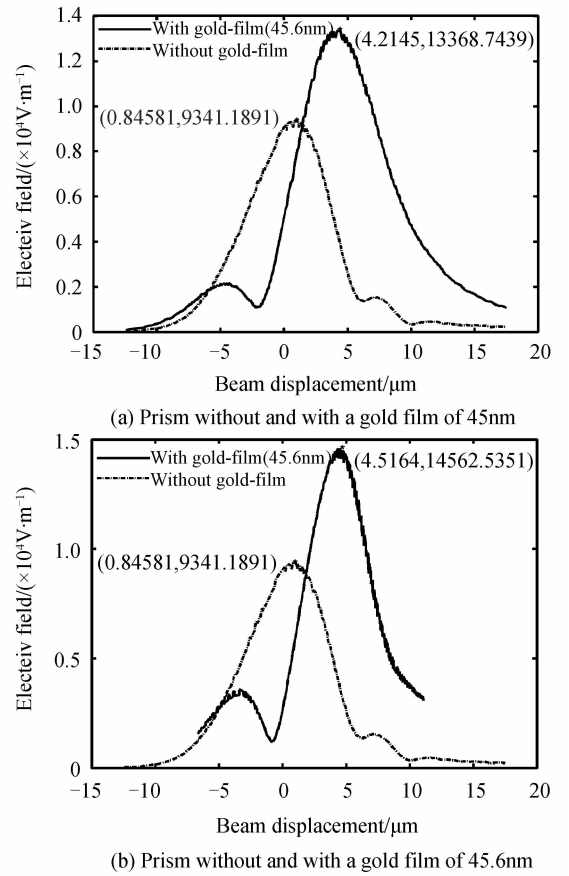

Fig. 7 *E*-field intensity distributions of optical-mode propagations

For the isosceles triangle prism, by comparing the position appeared the maximum *E*-field intensity at prism coated with a gold film of 45 nm with that of the prism without gold film, the beam displacement obtained by using CM, at different incident angle, are shown in Table 1.

Table 1 Beam displacement vs. incident angle

Angle/(°)	Beam displacement/μm
43.6	+2.95
43.8	+3.14
43.9	+3.28
44.1	+3.37
44.2	+3.29
44.3	+3.21
44.4	+3.15

From Table 1, around the resonance angle of 44.1°, the beam displacement is positive. The thickness (45 nm) of the gold film is less than the critical thickness (45.8 nm); the resonance absorption cannot be balanced by radiation damping and internal damping[6]. Therefore, under the particular condition of radiation damping, the total flux of reflected light is larger than the negative flux in the gold film[9], which leads to forward surface-propagating energy along the gold-air interface, resulting in a positive GH shift, the maximum beam displacement of +3.37 μm is found by using CM at an incident angle of 44.1°. The positive GH shifts obtained using CM are in agreement with those obtained by the SPA around the resonance angle, although the enhancement effect using CM was much less than that using SPA.

3 Conclusion

In conclusion, the positive and negative GH shifts were found when the thickness of the gold film is less than and greater than critical thickness, respectively. The results indicate the forward and backward surface-propagating energy flowing along the gold-air interface at SPR. When the thickness of gold film is less than the critical thickness, radiation damping and internal damping cannot be used to balance the resonance absorption, making GH shift positive. For example, when the gold film thickness is 45 nm, the maximum beam displacement of +3.37 μm is found by using CM at an incident angle of 44.1°. These results, obtained using CM, is in agreement with that obtained using SPA around the resonance angle, although the enhancement effect using CM was much less than that using SPA, and indicates that the drastic phase changes at the resonance angle make SPA difficult for application in waveguide-type SPR devices, with sizes in the order of micro millimeter. These results are important for designing high-sensitivity SPR sensors and GH shift measurement as well as for application in waveguide-type SPR devices, with sizes in the order of micro millimeter.

References

[1] GOOS F, HÄNCHEN H. A new and fundamental experiment on total reflection[J]. *Annals of Physics*, 1947, **1**: 333-346.

[2] RENARD R H. Total reflection: A new evaluation of the Goos-Hänchen shift[J]. *Journal of the Optical Society of America*, 1964, **54**(10): 1190.

[3] ARTMANN K. Seitenversetzung der Berechnung des total reflek-tierten Stranles[J]. *Annals of Physics*, 1948, **2**: 87-102.

[4] YANG Xiao-yan, LIU De-ming, XIE Wen-cong, *et al*. High-sensitivity sensor based on surface plasmon resonance enhanced lateral beam displacements[J]. *Chinese Physics Letters*, 2007, **24**(2): 458-461.

[5] LI Chun-fang, YANG Xiao-yan. Thin-film enhanced Goos-Hänchen shift in total internal reflection[J]. *Chinese Physics Letters*, 2004, **21**(2): 485-488.

[6] YIN Xiao-bo, HESSELINK L, LIU Zhao-wei, *et al*. Large positive and negative lateral optical beam displacements due to surface plasmon resonance [J]. *Applied Physics Letters*, 2004, **85**(3): 372-374.

[7] YIN Xiao-bo, HESSELINK L. Goos-Hänchen shift surface

plasmon resonance sensor[J]. *Applied Physics Letters*, 2006, **89**(26): 261108.

[8] HOMOLA J, YEE S S, GAYGLITZ G. Surface plasmon resonance sensors: Review[J]. *Sensors and Actuators B*, 1999, **54**(1-2): 3-15.

[9] GEUM Y O, DOO G K, YOUNG W C. The characterization of GH shifts of surface plasmon resonance in a waveguide using the FDTD method[J]. *Optics Express*, 2009, **17**(23): 20714-20.

[10] KRETSCHMANN E, RAETHER H. Radiative decay of non-radiative surface plasmon excited by light[J]. *Zeitschrift fur Naturforschung A*, 1968, **23**(21): 35-36.

[11] ZHANG Zhi-wei, WEN Ting-dun, WU Zhi-fang. A novel method for heightening sensitivity of prism coupler-based SPR sensor[J]. *Chinese Physics Letters*, 2011, **28**(5): 054211.

[12] LI Song-quan, GAO Lai-xu, LIU Shu-guang, *et al*. Design of transverse magnetic-reflected polarizing film[J]. *Chinese Physics Letters*, 2014, **12**(5): 053102.

[13] NELSON S G, JOHNSTON K S, YEE S S. High sensitivity surface plasmon resonance sensor based on phase detection [J]. *Sensors and Actuators B*, 1996, **35**(1-3): 187-191.

[14] BORN M, WOLF E. Principle of optics[M]. Cambridge: United Kingdom at the University Press, 1997.

[15] CHEN Qiang-hua, LUO Hui-fu, WANG Su-mei, *et al*. Measurement of air refractive index based on surface plasmon resonance and phase detection by dual-frequency laser interferometry[J]. *Optics Letters*, 2012, **37**(14): 2916-8.

[16] LI Zhi-quan, MENG Xiao-yun, PIAO Rui-qi, *et al*. Humidity detection based on surface plasmon resonance[J]. *Acta Photonica Sinica*, 2015, **44**(6): 0624001.

[17] BERMAN P R. Goos-Hänchen shifts in negatively refractive media[J]. *Physical Review E*, 2002, **66**(6): 067603.